Results in Chemistry 4 (2022) 100655

Contents lists available at ScienceDirect

Results in Chemistry

journal homepage: www.sciencedirect.com/journal/results-in-chemistry

Highly efficient magnetically separable Zn-Ag@L-arginine Fe_3O_4 catalyst for synthesis of 2-aryl-substituted benzimidazoles and multicomponent synthesis of pyrimidines

Padmakar A. Kulkarni [a], Sandeep S. Kahandal [b], Nitin A. Mirgane [c], Ashis Kumar Satpati [d], Suresh S. Shendage [a,*]

[a] Department of Chemistry, KET'S Vinayak Ganesh Vaze, College of Arts, Science and Commerce, (Autonomous), Mithagar Road, Mulund (E), Mumbai 400081, India
[b] Department of Chemistry, VPM's B. N. Bandodkar College of Science, (Autonomous) Jnanadweepa, Chendani Bunder Road, Thane (W), Thane 400601, India
[c] Post Graduate Department of Chemistry, SIES College of ASC, Sion (West) affiliated to University of Mumbai, Mumbai 400 022, India
[d] Analytical Chemistry Division, Bhabha Atomic Research Centre, Homi Bhabha National Institute, Trombay, Mumbai 400 085, India

ARTICLE INFO

Keywords:
Zn-Ag @L-arginine Fe_3O_4
Benzimidazole
Pyrimidine
Magnetic Nanocatalyst

ABSTRACT

A general and efficient one pot protocol has been developed for the synthesis of benzimidazoles and pyrimidines using Zn and Ag@L-arginine Fe_3O_4 as a heterogeneous catalyst. The prepared catalyst provided good yields of the corresponding products within a short reaction time. Catalyst was characterized by using XRD, TEM, FEG-SEM, EDS, XPS, Raman, CHNS and FT-IR. The present method provided high yields of the products with wide substrates scope. The catalyst could be reused five cycles without a significant loss of catalytic activity.

Introduction

During the last few decades, magnetically separable materials area emerged as notable tool for organic transformations due to their properties like easy separation, recyclability, and nonleaching nature of the catalyst in the reaction medium. These materials are used in a variety of fields, including administration of drugs, magnetic high-density information storage, magnetic resonance imaging, and cancer treatment [1]. Their magnetic features, prevent material loss and increases cost-effectiveness, making them appealing industrial-scale alternatives [2]. Magnetite, a type of magnetic material, is extensively studied for the creation of more environmentally benign reaction protocols, and the field is still productive for research [3].

Magnetic nanoparticle-based materials are being extensively explored as a green chemistry tool in organic synthesis, since they are easy to prepare, cost-effective, and environmentally friendly [4]. Heterocyclic compounds, which are made up of carbon, nitrogen, and oxygen, are used in a wide range of potent drugs. The 2-aryl-substituted benzimidazoles and pyrimidines are found in pharmacologically active compounds and natural products [5,6]. These compounds are extensively used as antiviral, antimicrobial, antibiotic, antifungal, anticonvulsant, antiulcer, analgesic, antihypertensive agents, [7] also light-emitting devices [8]. Benzimidazole derivatives act as effective fungicides [9] and also exhibit distinct pharmaceutical properties such as Telmisartan as AT_1 receptor antagonists and Rabeprazole used in the treatment of gastric ulcers [10,11]. Oxibendazole, Albendazole,and Mebendazole to treat parasitosis, bis benzimidazole derivatives bind with DNA topoisomerase, also cytotoxic against breast adenocarcinoma [12,13]. Tetrahydropyrimidine derivatives exhibit powerful and selective activities on a wide range of membrane receptors [14] and substituted derivatives of tetrahydropyrimidine are valuable building blocks for the synthesis of heterocycles that possess high activities towards cell-permeable antitumor scaffold, Monastrol, and antihypertensive agent (R)[15–17].

As a result, the development of novel synthetic methods for these heterocyclic molecules is crucial. In the last few decades, several elegant strategies for the synthesis of benzimidazoles derivatives have been well established by reacting 1,2 phenylenediamine with aldehyde/ carboxylic acids by using various catalysts such as $Fe_3O_4@SiO_2@(CH_2)_3N^+Me_3I_3^-$,[18] clay supported titanium catalyst,[19] lanthanum chloride,[20] NaY zeolite, [21] ceric ammonium nitrate/polyethylene glycol,[22] $CoFe_2O_4$, [23] DDQ [24]. However, in most of the earlier reports including ferrite and metals supported on ferrite catalysts, have drawbacks like longer reaction times, and high reaction temperatures

---

* Corresponding author.
E-mail address: sureshsshendage@gmail.com (S.S. Shendage).

https://doi.org/10.1016/j.rechem.2022.100655
Received 9 June 2022; Accepted 10 November 2022

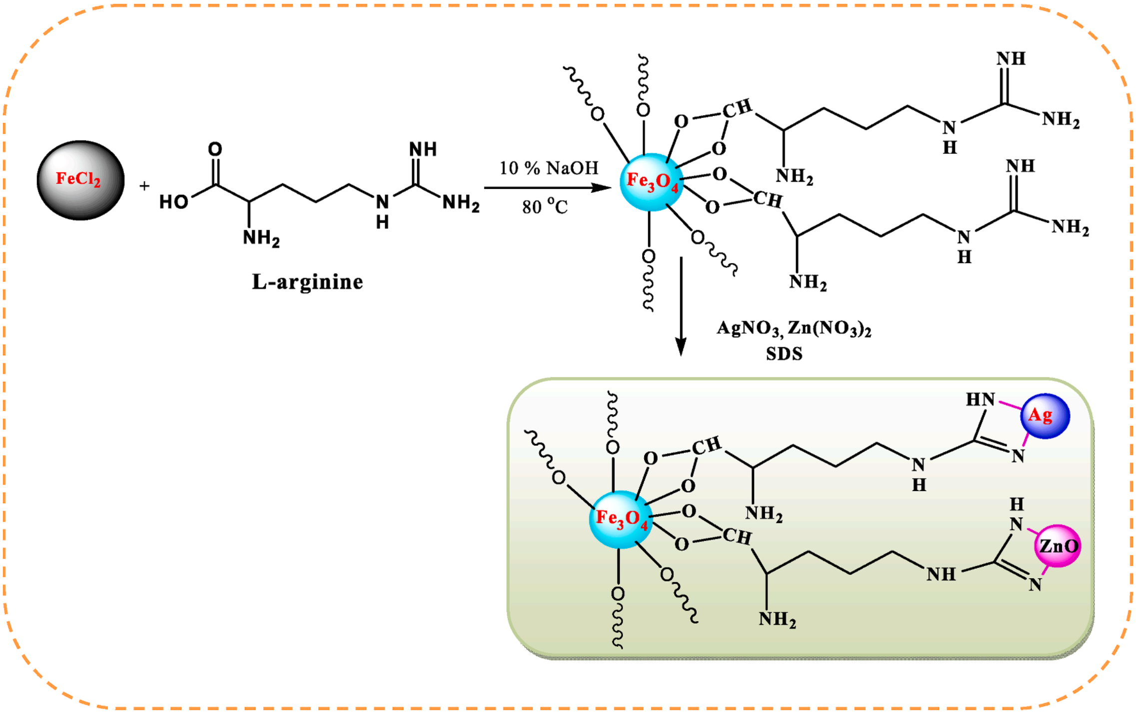

Scheme 1. Preparation of Zn-Ag @L-arginine Fe_3O_4 Catalyst.

with costly and tedious catalyst preparation procedures. Similarly, the synthesis of pyrimidine is generally carried out using aldehyde, urea, and β-ketoester in presence of acid catalysts such as $ZrOCl_2{\cdot}8H_2O$, [25] carrageenan moss/Fe_3O_4, [26] $Fe_3O_4@C@OSO_3H$, [27] ionic-liquid like $TiCl_3OTf$-[bmim]Cl, [28] Iron (III) Tosylate, [29] Cp_2TiCl_2 [30] and many more associated with some drawbacks of higher reaction temperatures, high catalyst loadings, and non-green protocols.

The heterogeneous catalysis finds numerous applications in the preparation of important oxygen and nitrogen containing heterocycles. Their use in biologically active pharmaceuticals, agrochemicals, and functional materials is increasingly becoming more and more important [31–37]. In continuation of our efforts for the development of environmentally benign and efficient routes for various organic functional group transformations [38–43]. In the present study, L-arginine serves as a bridge between ferrite Fe_3O_4 and ZnO-Ag nanoparticles in a Zn-Ag@L-arginine Fe_3O_4 catalyst. In the present catalytic system, ZnO plays an important role as a Lewis acid catalyst [44] and Ag metal [45,46] for the activation of carbonyls and also plays a vital role in the transition states of reaction mechanisms like dehydration, oxidation, and cyclization. ZnO and silver metal enhance the catalytic activity of the material.

To the best of our knowledge, the synthesis of 2-aryl-substituted benzimidazoles and pyrimidines using a recyclable and magnetically separable heterogeneous catalyst Zn-Ag @L-arginine Fe_3O_4 was not previously documented in the literature.

Experimental

Chemicals

All chemicals and reagents were procured with the maximum purity obtainable from S.D. Fine Chemicals and utilized without further purification.

Characterization

Powder X-ray diffraction (XRD) was performed on a PANalytical, X' Pert Pro diffractometer using Cu/Kα radiation with a wavelength of 1.54184 Å in the range of 2θ range of 25–90°. Scanning electron microscopic (SEM) images and EDS were collected on a JEOL JSM-7600F FEG-SEM microscope. Transmission electron microscopy (TEM) was performed with a PHILIPS CM 200 instrument (Operating voltages: 20-200kv). FT-IR spectra of samples were investigated on a 3000 Hyperion Microscope with Vertex 80 FTIR System (Bruker, Germany). X-ray photoelectron spectroscopy of the catalyst was recorded on a Thermo Fischer Scientific ESCALAB Xi + instrument and Raman spectra were studied with Raman-Horiba Japan Xplora Plus. Elemental analysis was investigated using Thermo Scientific, FlashSmart Elemental Analyzer. ^{1}H and ^{13}C NMR spectra were recorded on a Bruker Avance III, 400 MHz, NMR instrument in DMSO-d_6 with TMS as the standard.

Catalyst preparation:

The catalyst Zn-Ag@L-arginine Fe_3O_4 (Scheme 1), was prepared according to a previously reported procedure with some modifications [47]. In a typical experiment, 100 mL of an aqueous 20 mM $FeCl_2$ solution was stirred with 100 mL aqueous solution of 20 mM L-arginine solution under a nitrogen atmosphere at 10 °C, with the constant addition of 10 % NaOH solution to make the pH of the reaction mass 11 to 12. The prepared material was heated to 80 °C for 1.5 h. further cooled at room temperature and filtered. The resulting solid material (Arginine ferrite) was then washed with pure water followed by ethanol and dried at 50 °C in an oven under a vacuum. In 100 mL round bottom assembly 1.0 g Arginine ferrite (solid material) with 0.6 g of $Zn(NO_3)_2$ and 0.2 g of $AgNO_3$ with 10 % SDS (Sodium dodecyl sulfate) in 50 mL water sonicated for 1.5 h. The pH of the resultant solution maintains at 10 to 11 by adding hydrazine hydrate and heating for 3 h at 80 °C. The resultant material cooled for 1.5 h at room temperature and filtered solid material was washed with water followed by ethanol.

Typical experimental procedure:

General procedure for the synthesis of 2-aryl-substituted benzimidazoles:

The Zn-Ag@L-arginine Fe_3O_4 (5 mol%) catalyst was added to a solution of o-phenylenediamine (1 mmol) and aldehyde (1 mmol) in 5 mL

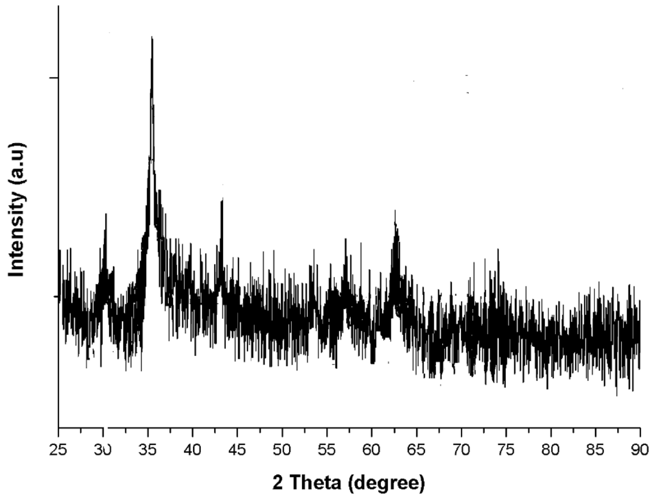

Fig. 1. XRD of Zn-Ag@L-arginine Fe_3O_4.

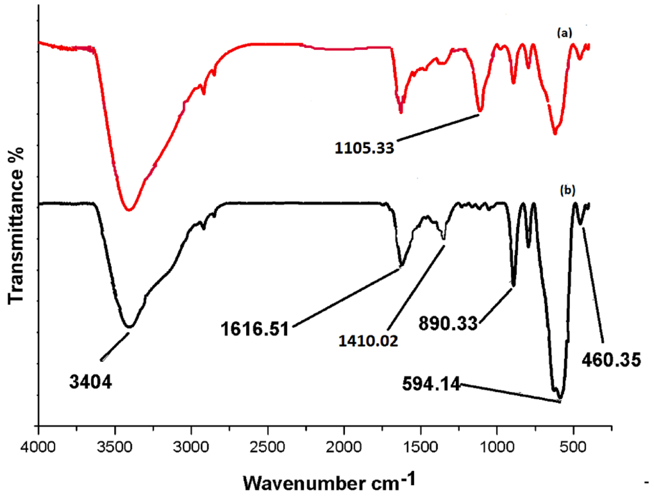

Fig. 2. FT-IR spectra of (a) arginine Fe_3O_4 (b) Zn-Ag@L-arginine Fe_3O_4.

of ethanol. The mixture was stirred and heated at 65 °C for 20–45 min. and reaction progress was monitored by using TLC. After completion of the reaction, the catalyst was recovered using an external magnet. The reaction mixture was quenched and extracted with dichloromethane (25 mL) and washed with water. The organic phase was separated, dried on Na_2SO_4 and concentrated in a vacuum to get the crude solid. The crude compounds were purified by silica gel column chromatography.

General procedure for the synthesis of pyrimidines:. The Zn-Ag@L-arginine Fe_3O_4 (5 mol %) catalyst was added to a solution of aldehyde (1 mmol), urea (1 mmol) and ethyl acetoacetate (1 mmol), in 5 mL of ethanol. The mixture was stirred and heated at 45 °C temp. for 30–60 min. and reaction progress was monitored by using TLC. After completion of the reaction, the catalyst was recovered using an external magnet. The reaction mixture was quenched and extracted with dichloromethane (25 mL) and washed with water. The organic phase was separated, dried on Na_2SO_4, and concentrated in a vacuum to get the crude solid. The crude compounds were purified by silica gel column chromatography.

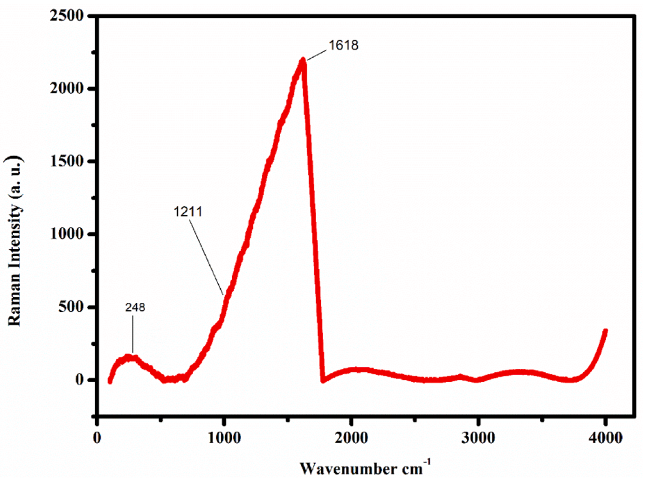

Fig. 3. Raman spectra of Zn-Ag@L-arginine Fe_3O_4.

Results and discussion

Characterization of catalyst

X-ray diffraction (XRD)

The structural analysis of the Zn-Ag@L-arginine Fe_3O_4 was investigated by using powder X-ray diffraction (XRD) in the range of 2θ between 25° to 90°. From the XRD pattern of the catalyst (Fig. 1), it can be observed that all the reflection peaks match well with the standard lattice parameter of magnetite nanoparticles. Strong diffraction peaks at 2θ of 30.10°, 35.48°, 43.15°, 53.47°, 56.97°, and 62.43° belong to the peaks of (220), (311), (400), (422) (511) and (440) of the Fe_3O_4(JCPDS card No. 19–0629) [48,49]. Due to the low percentage of Zn (6.01 % by EDS) and Ag (0.46 % by EDS), the peaks of Zn and Ag are not detectable in the XRD spectrum [3]. The average particle size of nanoparticles obtained was 27 nm using the Scherrer equation.

FT-IR and Raman spectra

The FT-IR spectrum of Zn-Ag@L-arginine Fe_3O_4 in the spectral range from 400 to 4000 cm^{-1} is shown in Fig. 2 **(a-b).** The Fe-O lattice vibration is characterized by a prominent IR band at around 594 cm^{-1} (Fig. 2**b**) [50], while the N—H stretching vibrations at 3404 cm^{-1} and the bending mode of the free NH_2 group at 1616 cm^{-1} confirm arginine coating (Fig. 2**b**) [51]. IR peaks in the region of 760–1180 cm^{-1}, mainly due to the C—C stretching and C—N stretching vibrations in the catalyst [52]. The low intensity peak formed at 1410 cm^{-1} which indicates the symmetric stretching of the CO_2^-. An absorption band was observed at around 460 cm^{-1}; which corresponds to the shifting of the $\nu 2$ band of the Fe–O bond of magnetite to a higher wavenumber [51]. Thus, confirming the existence of arginine molecules on nanoparticle surfaces. As a result, magnetite nanoparticles are stabilized by arginine via the carboxyl group, forming an attachment of the arginine to the magnetite particle.

The Raman spectra of the Zn-Ag@L-arginine Fe_3O_4 (Fig. 3) show a strong peak at 1618 cm^{-1} assigned to mainly antisymmetric stretching of the CO_2^- group. The weak band appeared at 1211 cm^{-1} assigned to the wagging mode of the NH_2 group of the arginine [53]. The spectrum shows a sharp band at 248 cm^{-1}, ascribed to the stretching vibrations of Ag–N which confirms the formation of silver nanoparticles [46,54].

FEG-SEM

The surface morphology of Zn-Ag@L-arginine Fe_3O_4 heated for 3 hr. at 80 °C was characterized by using the scanning electron microscopy technique. The SEM micrographs of Zn-Ag @L-arginine Fe_3O_4 results as shown in Fig. 4 a-c. EDS confirms the presence of Zn and Ag metals in the prepared nanomaterial (Table 1, Fig. 4 d).

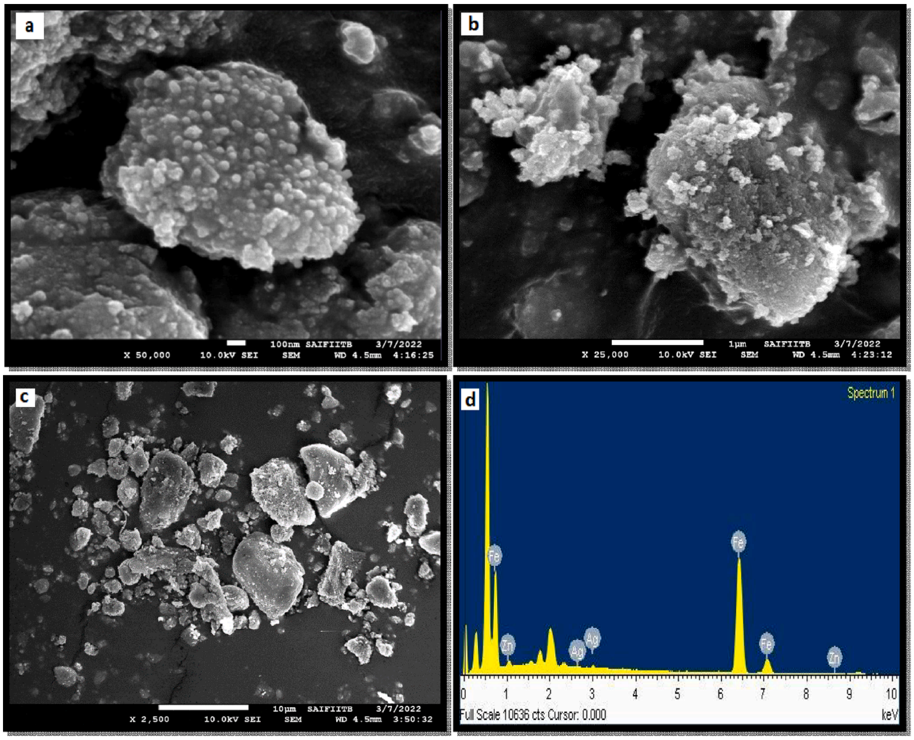

Fig. 4. (**a-c**) FEG-SEM image of Zn-Ag@L-arginine Fe_3O_4, (**d**)EDS profile of Zn-Ag@L-arginine Fe_3O_4.

Table 1
Elemental composition of the Zn-Ag @L-arginine Fe_3O_4.

No.	Element	Weight%	Atomic%
1	Fe	92.20	93.54
2	Zn	6.93	6.01
3	Ag	0.87	0.46

Transmission electron microscopy (TEM)

A TEM micrograph of Zn-Ag@L-arginine Fe_3O_4 was acquired to obtain additional information on particle size and shape. The TEM images of Zn-Ag @L-arginine Fe_3O_4 results confirm the formation of Fe_3O_4 nanoparticles. (Fig. 5, a-d) In XRD analysis an average particle size was calculated and found to be 27 nm using the Scherrer equation.

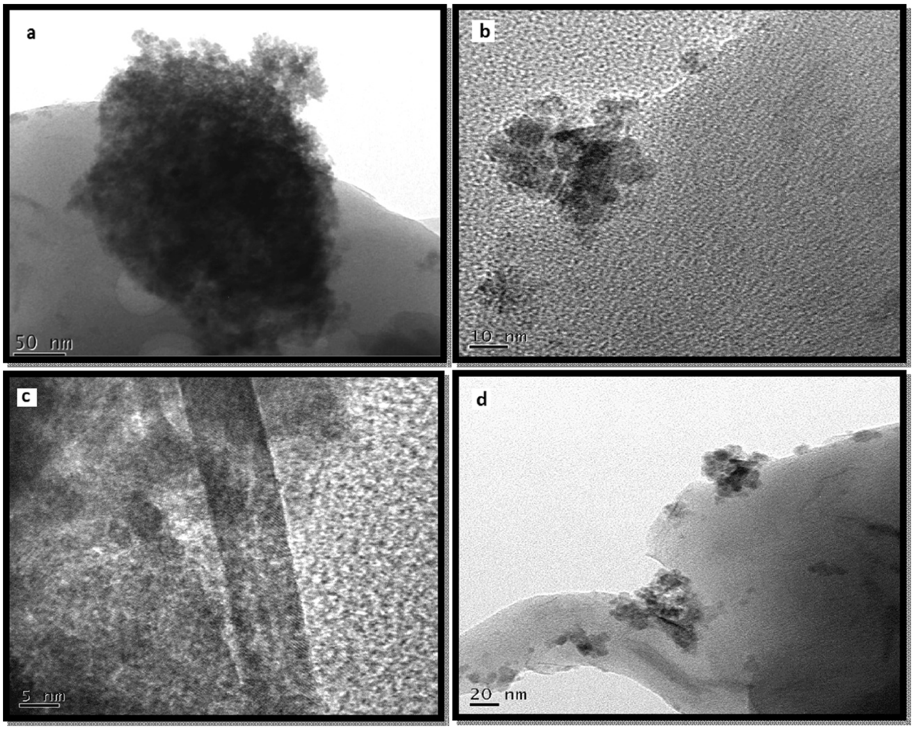

Fig. 5. (**a-d**) TEM of Zn-Ag @L-arginine Fe_3O_4.

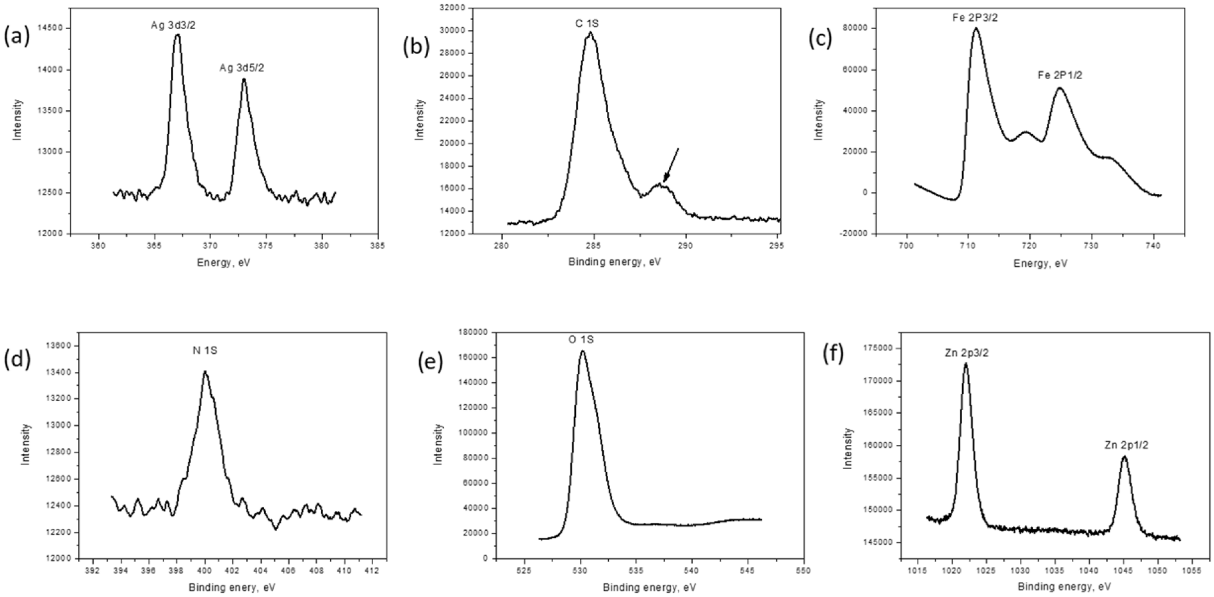

Fig 6. XPS spectra of Zn-Ag@L-arginine Fe_3O_4 catalyst **(a)** Ag 3 d, **(b)** C 1 s, **(c)**Fe 2p, **(d)**N 1 s,**(e)**O1s, **(f)**Zn 2p.

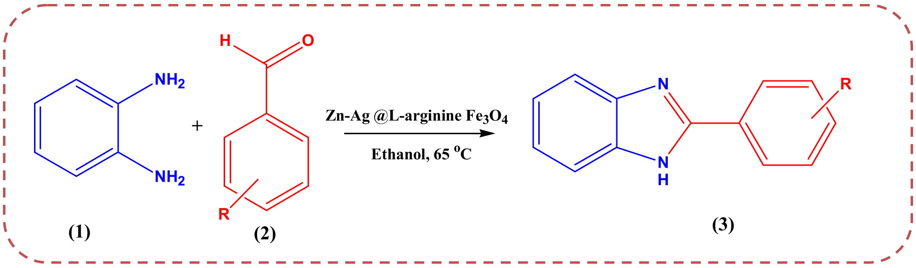

Scheme 2. Synthesis of 2-aryl-substituted benzimidazoles catalyzed by Zn-Ag @L-arginine Fe_3O_4.

X-ray photoelectron spectra

The results of the XPS measurements are shown in Fig. 6. After getting an idea about the elemental profile the high-resolution spectra of Ag, C, Fe, N, O and Zn are shown in the plot. The peaks for both Ag $3d_{5/2}$ and Ag $3d_{3/2}$ appeared in spectra with a peak separation of 5.9 eV indicating the formation of metallic silver [55,56]. The XPS peak of C 1 s is characterized with the peak at its usual position, additionally, the peak at around 288 eV is indicative of the presence of functionalized carbon. The XPS spectra of Fe has been characterized with two peaks Fe $2p_{3/2}$ and Fe $2p_{1/2}$, additionally, a satellite peak has been observed at around 719 eV. In the O 1s spectra, the peak can be seen with a hump at 532 eV, which is indicative of the oxygen present as C=O. The XPS peaks for N and Zn are observed at their usual position. The peaks of both Zn $2p_{1/2}$ and Zn $2p_{3/2}$ appeared in spectra with bonding energies difference of 23.15 eV suggesting + 2 oxidation state of zinc [56,57].

Catalytic activity studies:

Initially, in order to explore the applicability of Zn-Ag@L-arginine Fe_3O_4 catalyst, the model reaction of o-phenylenediamine **1** and aldehyde **2** (1.0 mmol each) for the synthesis of benzimidazoles **3** (Scheme 2) was carried out. In case of heterogeneous catalyzed reactions, catalyst concentration is one of the most important factors and hence, we have screened the amount of catalyst required for the maximum yield of the product. It is noteworthy that, in the absence of a catalyst no significant product formation was observed even after an extended reaction time of 60 min (Table 2, entry 1). In presence of Zn-Ag @L-arginine Fe_3O_4 catalyst, 5 mol % amount was found to give 96 % yield of the desired product as compared to 2 mol% (Table 2, entries 2–3). Further, an increase of catalyst amount from 5 to 20 mol% shows a slight decrease in catalytic activity from 96 to 95 % yield of the product (Table 2, entries 4–5).

The effect of the temperature study revealed that product yield significantly increases when temperature increases from room

Table 2
Effect of various reaction conditions on the synthesis of 2-aryl-substituted benzimidazoles[a.]

Entry	Catalyst (mol %)	Solvent	Temp. (°C)	Time (min.)	Yield[b](%)
Effect of catalyst loading					
1	–	EtOH	65	60	20
2	2	EtOH	65	60	89
3	5	EtOH	65	30	96
4	10	EtOH	65	30	95
5	20	EtOH	65	30	95
Effect of temperature					
6	5	EtOH	r.t.	60	45
7	5	EtOH	45	60	68
8	5	EtOH	65	30	96
Effect of solvents					
9	5	solvent free	65	30	80
10	5	acetonitrile	65	30	56
11	5	CH_2Cl_2	Reflux	60	40
12	5	water	65	60	60
13	5	EtOAC	65	90	70

[a] Reaction conditions: benzaldehyde (1 mmol), o-phenyldiamine (1 mmol), solvent 5 mL, catalyst mol % (w.r.t. benzaldehyde), [b]Isolated yield.

Table 3
Reaction between various aldehydes and o-phenyldiamine catalyzed by Zn-Ag@L-arginine Fe_3O_4[a.]

Entry	R	Product	Time (min)	Yield[b](%)
1	H	3a	25	96
2	4-CH_3	3b	40	96
3	4-Cl	3c	20	98
4	4-Br	3d	30	95
5	4-F	3e	25	94
6	2-OH	3f	30	92
7	4-OH	3 g	25	97
8	2-OCH_3	3 h	30	93
9	4-OCH_3	3i	35	91
10	3-NO_2	3j	30	95
11	4-NO_2	3 k	20	98
12	-C_4H_4	3 l	45	91

[a] **Reaction conditions**: aldehyde (1 mmol), o-phenyldiamine (1 mmol), ethanol- 5 mL, temp-65 °C, catalyst – 5 mol %, (w.r.t. aldehyde),[b]Isolated yield.

temperature to 65 °C (Table 2, entries 6–8). The effect of the reaction medium was also evaluated with solvents such as acetonitrile, CH_2Cl_2, water, and EtOAc (Table 2, entries 10–13). Under solvent-free conditions, a good amount of product yield was obtained (Table 2, entry 9), whereas ethanol mediated reaction provided 96 % yield within 30 min. of reaction time (Table 2, entry 3).

To study the wide applicability of Zn-Ag@L-arginine Fe_3O_4, we have carried out a substrate study using structurally varied aldehydes. The catalyst afforded good to moderate product yields for both electrons donating (–CH_3, –OH, –OCH_3, -C_4H_4) and electron withdrawing (-Cl, -Br, –NO_2) substituents (Table 3, entries 1–12). In all cases, the reaction smoothly took place under optimized reaction conditions.

The applicability of the prepared catalyst was further explored for the synthesis of pyrimidines **7** by taking a mixture of aldehyde **4** (1 mmol), urea **5** (1 mmol), and ethyl acetoacetate **6** (1 mmol), in presence of Zn-Ag@L-arginine (Scheme 3). In the broad optimization study, the amount of catalyst was tested for the model reaction. In absence of a catalyst, no significant product formation was observed under the same set of conditions even after an extended reaction time of 90 min (Table 4, entry 1). An increase in catalyst loading from 2 to 5 mol % enhanced the product yield from 75 to 98 % (Table 4, entries 2–3). Further, an increase in catalyst loading had no remarkable effect on product yield (Table 4,entries 4–5). Thus 5 mol % of catalyst loading was selected as the optimum concentration for further studies (Table 4, entry 3). Similarly, temperature dependence was found for the model reaction, the optimum results were found at 45 °C in comparison to other temperatures evaluated (Table 4, entries 6–8).

The effect of solvents has been screened by using toluene, dichloromethane, water, and ethyl acetate (Table 4, entries 10–13). Interestingly in solvent free conditions, a moderate yield of 65 % was obtained for the model reaction (Table 4, entry 9). In ethanol mediated reaction highest 98 % yield of the desired product was furnished within 25 min of reaction time (Table 4, entry 3).

To check the versatility of the Zn-Ag@L-arginine Fe_3O_4, we have shown a wide substrate scope by using structurally diverse groups on aldehydes. The catalyst afforded a good to moderate product yield for both electrons donating (–CH_3, –OCH_3,) and electron withdrawing (-Cl, –NO_2) substituents on benzaldehyde (Table 5, entries 1–7). The reaction between, thiophene-2-carboxaldehyde, urea, and ethylacetoacetate also provided 91 % yield of the product within 45 min of reaction time (Table 5, entry 8). However, in most cases, benzaldehydes containing electron withdrawing groups took a long time to complete the reaction.

Based on the results of these experiments, a plausible reaction pathway for the synthesis of benzimidazoles involves the formation of imine (c) in the first step via condensation of o-phenyldiamine (a) in presence of electron-deficient carbonyl carbon of aldehyde (b) activated by the silver metal sites [46] of Zn-Ag@L-arginine Fe_3O_4 with the removal of one H_2O molecule (Scheme 4**).** Furtherimine intermediate undergoes the ring closure by attachment of a nitrogen atom lone pair to Lewis acid sites of the catalyst (ZnO) to form unstable benzimidazoline (d) [24].Then, two hydrogen atoms were removed in the presence of silver metal from the catalysts and finally, benzimidazole derivatives (e) were prepared [58]. However, further study is needed to support the

Table 4
Effect of various reaction conditions on the synthesis of pyrimidines[a.]

Entry	Catalyst (mol %)	Solvent	Temp. (°C)	Time (min.)	Yield[b](%)
Effect of catalyst loading					
1	–	EtOH	45	90	34
2	2	EtOH	45	45	75
3	5	EtOH	45	25	98
4	10	EtOH	45	30	98
5	20	EtOH	45	30	98
Effect of temperature					
6	5	EtOH	r.t.	30	42
7	5	EtOH	45	25	98
8	5	EtOH	65	30	96
Effect of solvents					
9	5	solvent free	45	25	65
10	5	toluene	45	60	85
11	5	CH_2Cl_2	Reflux	80	70
12	5	water	45	40	65
13	5	EtOAc	45	140	89

[a] **Reaction conditions**: benzaldehyde (1 mmol), ethylacetoacetate (1 mmol), urea (1 mmol), solvent- 5 mL, catalyst mol % (w.r.t. benzaldehyde), [b]Isolated yield.

Table 5
Three component reaction between various benzaldehyde, ethylacetoacetate, and urea catalyzed by Zn-Ag@L-arginine Fe_3O_4[a.]

Entry	R	Product	Time (min)	Yield[b](%)
1	C_6H_5	7a	30	98
2	4-CH_3-C_6H_4	7b	40	96
3	2-Cl-C_6H_4	7c	55	95
4	4-Cl-C_6H_4	7d	30	96
5	4-OCH_3-C_6H_4	7e	45	97
6	3-NO_2-C_6H_4	7f	60	93
7	4-NO_2-C_6H_4	7 g	40	95
8	C_4H_3S	7 h	45	91

[a] **Reaction conditions**: aldehyde (1 mmol), ethylacetoacetate (1 mmol), urea (1 mmol), ethanol- 5 mL, temp- 45 °C, catalyst – 5 mol %, (w.r.t. aldehyde), [b]Isolated yield.

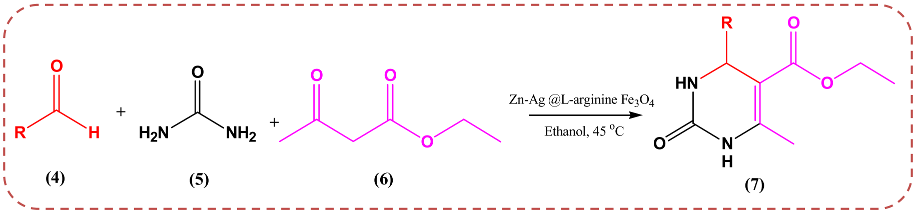

Scheme 3. Multicomponent synthesis of pyrimidines catalyzed by Zn-Ag@L-arginine Fe_3O_4.

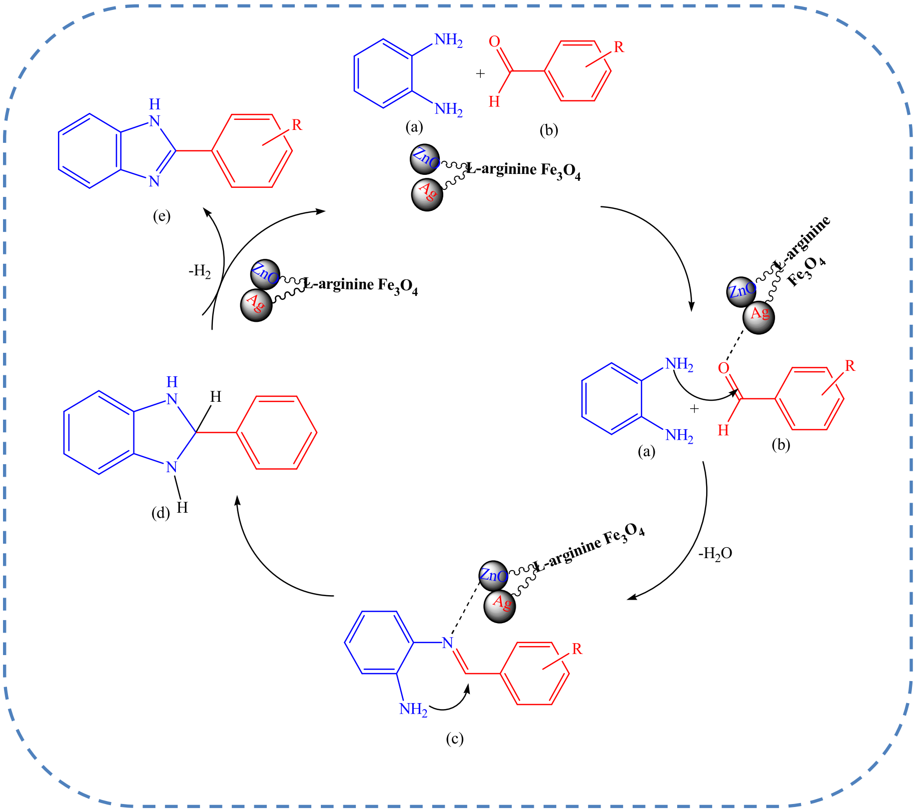

Scheme 4. A plausible reaction mechanism for the synthesis of benzimidazoles.

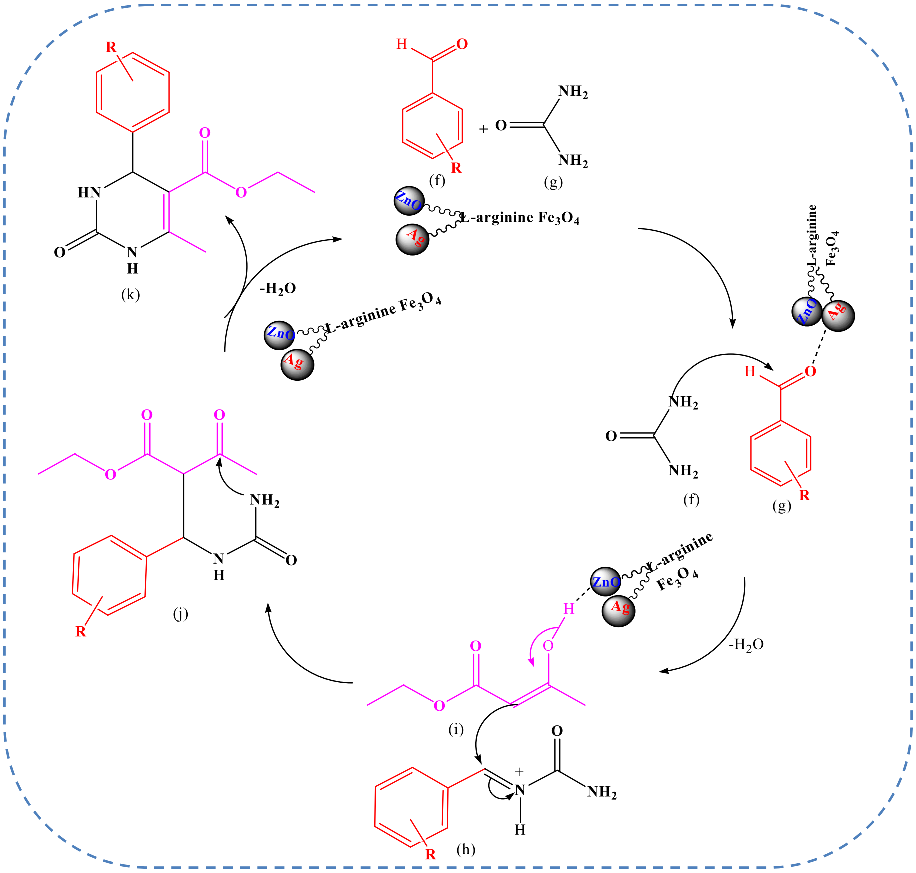

Scheme 5. Proposed reaction pathway for synthesis of pyrimidines catalyzed by Zn-Ag@L-arginine Fe_3O_4.

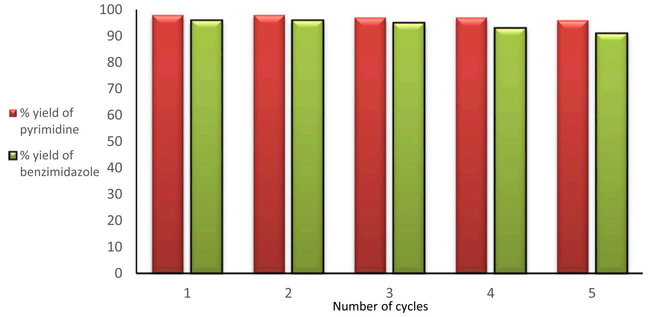

Fig. 7. Recyclability study of Zn-Ag @L-arginine Fe_3O_4.

Table 6
Comparison of the present work with some reported methods for the synthesis of benzimidazoles.

No.	Catalyst and Conc.	Time	Yield (%)	Temperature (°C)	Reference
1	$Fe_3O_4@SiO_2@(CH_2)_3N^+Me_3I_3^-$, (0.007 g for 1 mmol of OPD)	13–20 min	88–94	100 °C	18
2	Clay-supported titanium catalyst, (0.25 g for 1 mol of OPD)	2 h	62–82	120 °C	19
3	Lanthanum Chloride (10 mol %)	2–4 h	85–95	r.t	20
4	NaY Zeolite (100 mg for 0.0025 mol of OPD)	48 h	26–93	r.t.	21
5	Ceric ammonium nitrate/ polyethylene glycol (5 mol %)	1.5–3 h	90–98	50 °C	22
6	$CoFe_2O_4$ (5 mol%), grinding	7–11 min	88–97	–	23
7	Zn-Ag @L-arginine Fe_3O_4(5 mol %,w.r.t. aldehyde)	20 – 40 min	91–98	65 °C	**Present work**

Table 7
Comparison of the present work with some reported methods for the synthesis of pyrimidines.

Sr. No	Catalyst and conc.	Time	Yield (%)	Temperature	Reference
1	Magnetic core–shell Carrageenan moss/ Fe_3O_4(10 mg for 1 mmol of aldehyde)	45–90 min.	73–95	H_2O-Reflux	26
2	$Fe_3O_4@C@OSO_3H$ (8.1 mol%)	15–105 min	80–97	80 °C	27
3	$TiCl_3OTf$-[Bmim]Cl (15 % mol)	15–40 min	70–95	140 °C	28
4	Iron (III) Tosylate (5 mol%)	2.5 – 43 h	62–9	70–125 °C	29
5	Cp_2TiCl_2 (0.1 mmol)	9 h	12–93	70 °C	30
6	Zn-Ag @L-arginine Fe_3O_4(5 mol %w.r.t. aldehyde)	30–60 min	91–98	45 °C	**Present work**

postulated reaction mechanism.

The possible reaction mechanism of pyrimidine synthesis catalyzed by Zn-Ag@L-arginine Fe_3O_4 as a catalyst is depicted in Scheme 5. The reaction between benzaldehyde (f) and urea (g) generates iminium cation (h) via the addition of urea to electron-deficient carbonyl carbon of aldehyde (b) activated by the silver metal sites [46] of the catalyst. Subsequently, the addition of 1,3 dicarbonyl compound (i) with iminium cation (h) to form (j), which on cyclization and dehydration forms the corresponding product (k) in presence of Lewis acid sites of the catalyst. Following the formation of the product, the catalyst is free to participate in the next catalytic cycle [59]. However, further investigation is required to confirm the proposed reaction mechanism and synergetic effect of Ag and ZnO may play an important role in the reaction.

The reusability of catalysts is an important factor in determining the industry's potential applications. The recyclability of the catalyst was studied for five successive cycles for the synthesis of benzimidazoles and pyrimidines (Fig. 7). During the investigation, it was observed that the catalyst could be successfully separated and recycled by using a magnet without diminishing any catalytic activity. These results reveal that the given approach is effective and has several advantages over earlier protocols.

The study was further extended to confirm the heterogeneous nature of the catalyst by a hot filtration method. Both model reactions were carried out using optimized reaction conditions and the reaction mass was separated from the catalysts after 10 min of reaction time. The reaction mass was subsequently agitated for further 60 min without catalysts, and no further product formation was noted, showing the heterogeneous nature of the catalyst.

The current methodology for the synthesis of benzimidazole (Table 6) and pyrimidine (Table 7) is compared with some of the reported methods in the literature, and it is concluded that the present protocol offered a valuable improvement over the existing techniques.

Conclusion:

In summary, we have developed a green and efficient protocol for the synthesis of 2-aryl-substituted benzimidazoles and pyrimidines in ethanol using a magnetically separable Zn-Ag@L-arginine Fe_3O_4 catalyst. The material shows remarkable activity tolerance for aldehydes with both electron withdrawing and donating substituents present on the aromatic compounds. The catalytic material can be easily retrieved by using a magnet and reused without further treatment up to five catalytic cycles without a remarkable decline in catalytic activity. The protocol outperforms previous approaches due to its simple work-up procedure, mild reaction conditions, magnetically separable material, and reusability of the catalyst, which make the protocol more attractive and a useful contribution to the present methodologies.

CRediT authorship contribution statement

Padmakar A. Kulkarni: Conceptualization, Methodology, Formal analysis. **Sandeep S. Kahandal:** Data curation, Writing – original draft. **Nitin A. Mirgane:** Visualization, Investigation. **Ashis Kumar Satpati:** Formal analysis. **Suresh S. Shendage:** Supervision, Writing – review & editing.

Declaration of Competing Interest

The authors declare that they have no known competing financial interests or personal relationships that could have appeared to influence the work reported in this paper.

Data availability

Data will be made available on request.

Acknowledgements

"Authors are thankful to KET'S V. G. Vaze College (Autonomous) Mumbai (India)" for providing necessary facilities.

Appendix A. Supplementary data

Supplementary data to this article can be found online at https://doi.org/10.1016/j.rechem.2022.100655.

References:

[1] S. Singamaneni, V.N. Bliznyuk, C. Binek, E.Y. Tsymbal, Magnetic nanoparticles: recent advances in synthesis, self-assembly and applications, J. Mater. Chem. 21 (2011) 16819–16845, https://doi.org/10.1039/C1JM11845E.

[2] Y. Zheng, P.D. Stevens, Y. Gao, Magnetic nanoparticles as an orthogonal support of polymer resins: applications to solid-phase Suzuki cross-coupling reactions, J. Organomet. Chem. 71 (2006) 537–542, https://doi.org/10.1021/jo051861z.

[3] M.B. Gawande, V.D.B. Bonifácio, R.S. Varma, I.D. Nogueira, N. Bundaleski, C.A. A. Ghumman, O.M.N.D. Teodoro, P.S. Branco, Magnetically recyclable magnetite-ceria (Nanocat-Fe-Ce) nanocatalyst–applications in multicomponent reactions under benign conditions, Green Chem. 15 (5) (2013) 1226.

[4] A. Dandia, V. Parewa, A.K. Jain, K.S. Rathore, ZnS nanoparticle-catalyzed synthesis of spirooxindole derivatives in aqueous medium via Knoevenagel condensation followed by Michael addition, Green Chem. 13 (2011) 2135–2145, https://doi.org/10.1039/C1GC15244K.

[5] E. Vitaku, D.T. Smith, J.T. Njardarson, Analysis of the Structural Diversity, Substitution Patterns, and Frequency of Nitrogen Heterocycles among U.S. FDA Approved Pharmaceuticals, J. Med. Chem. 57 (2014) 10257–10274, https://doi.org/10.1021/jm501100b.

[6] J. Muškinja, N. Janković, Z. Ratković, G. Bogdanović, Z. Bugarčić, Vanillic aldehydes for the one-pot synthesis of novel 2-oxo-1,2,3,4-tetrahydropyrimidines, Mol. Divers. 20 (3) (2016) 591–604, https://doi.org/10.1007/s11030-016-9658-y.

[7] M. Faheem, A. Rathaur, A. Pandey, V. Kumar Singh, A.K. Tiwari, A Review on the Modern Synthetic Approach of Benzimidazole Candidate, ChemistrySelect 5 (2020) 3981–3994, https://doi.org/10.1002/slct.201904832.

[8] M. Hu, W. Song, J. Huang, Z. Xia, J. Su, Synthesis and device properties of carbazole/ benzimidazole-based host materials, Tetrahedron Lett. 58 (2017) 3583–3587, https://doi.org/10.1016/j.tetlet.2017.07.054.

[9] V. Srivastava, A.M. Srivastava, A.K. Tiwari, R. Srivastava, R. Sharma, H. Sharma, V. K. Singh, Disubstituted 4(3H) Quinazolones: A Novel Class of Antitumor Agents, Chem. Biol. Drug Des. 74 (2009) 297–301, https://doi.org/10.1111/j.1747-0285.2009.00850.x.

[10] K.J. McClellan, A. Markham, Telmisartan, Drugs 56 (1998) 1039–1044, https://doi.org/10.2165/00003495-199856060-00007.

[11] R. Srinivasulu, K.R. Kumar, P.V.V. Satyanarayana, Facile and Efficient Method for Synthesis of Benzimidazole Derivatives Catalyzed by Zinc Triflate, Green sustain. chem. 4 (2014) 33–37, https://doi.org/10.4236/gsc.2014.41006.

[12] C.E. Davila-Gutierrez, C. Vasquez, B. Trujillo-Hernandez, M. Huerta, Nitazoxanide compared with quinfamide and mebendazole in the treatment of helminthic infections and intestinal protozoa in children, Am. J. Trop. Med. Hyg. 66 (2002) 251–254, https://doi.org/10.4269/ajtmh.2002.66.251.

[13] Y. Huang, J. Zhou, Z. Xue, Y. Wu, J. Chen, H. Wu, M. Ji, Y. Shen, G. Cao, Z. Wu, G. Cao, Z. Wu, Y. Chen, K. Zheng, H. Zhu, M. Dai, H. Bao, Z. Shen, W. Hu, Z. Fang, G. Peng, M. Xu, R. Wang, Y. Tu, Clinical observations on the treatment of hookworm, ascaris and trichuris infection with oxibendazole, Chin J. Para. Paras. Dis. 8 (1990) 100–103.

[14] A.S. Alpan, S. Zencir, I. Zupko, G. Coban, B. Rethy, H.S. Gunes, Z. Topcu, Biological activity of bis-benzimidazole derivatives on DNA topoisomerase I and HeLa, MCF7 and A431 cells, J. Enzyme Inhib. Med. 24 (2009) 844–849, https://doi.org/10.1080/14756360802420831.

[15] C.O. Kappe, Biologically active dihydropyrimidones of the Biginelli-type-a literature survey, Eur. J. Med. Chem. 35 (2000) 1043–1052, https://doi.org/10.1016/S0223-5234(00)01189-2.

[16] K. Singh, D. Arora, S. Singh, Genesis of dihydropyrimidinone calcium channel blockers: recent progress in structure-activity relationships and other effects, Mini Rev. Med. Chem. (2009) 95–106, https://doi.org/10.2174/138955709787001686.

[17] P. Biginelli, Aldehyde-Urea Derivatives of Aceto- and Oxaloacetic Acids, Gazz Chim Ital 23 (1893) 360–413.

[18] E. Korani, K. Ghodrati, M. Asnaashari, Magnetic Core-Shell Nanoparticles Containing I−3 as a Novel Catalyst for the Facile Synthesis of Imidazole, Thiazole and Pyrimidine Derivatives in Solvent-Free Conditions, Silicon 10 (2018) 1433–1441, https://doi.org/10.1007/s12633-017-9623-0.

[19] V. Kannan, K. Sreekumar, Clay supported titanium catalyst for the solvent free synthesis of tetrasubstituted imidazoles and benzimidazoles, J. Mol. Catal. A Chem. 376 (2013) 34–39, https://doi.org/10.1016/j.molcata.2013.04.004.

[20] Y. Venkateswarlu, S.R. Kumar, P. Leelavathi, Facile and efficient one-pot synthesis of benzimidazoles using lanthanum chloride, Org. & Med. Chem. Lett. 3 (7) (2013) 1–8, https://doi.org/10.1186/2191-2858-3-7.

[21] A. Mobinikhaledi, N. Foroughifar, M. Zendehdel, M. Jabbarpour, Conversion of aldehydes to benzimidazoles using NaY zeolite, Synth. Reactivity Inorg. Metal-Org. Nano-Metal Chem. 38 (2008) 390–393, https://doi.org/10.1080/15533170802132261.

[22] M. Kidwai, A. Jahan, D. Bhatnagar, Polyethylene glycol: a recyclable solvent system for the synthesis of benzimidazole derivatives using CAN as catalyst, J. Chem. Sci. 122 (4) (2010) 607–612, https://doi.org/10.1007/s12039-010-0095-7.

[23] R.M. Borade, S.B. Kale, S.U. Tekale, K.M. Jadhav, R.P. Pawar, Cobalt ferrite magnetic nanoparticles as highly efficient catalyst for the mechanochemical synthesis of 2-aryl benzimidazoles, Catal. Commun. 159 (2021), 106349, https://doi.org/10.1016/j.catcom.2021.106349.

[24] H. Naeimi, Z. Babaei, Microwave-assisted practical and simple method for heterocyclization of o-phenylenediamine and aldehydes using DDQ as oxidant agent, Green Chem. Lett. Rev. 10 (2017) 129–133, https://doi.org/10.1080/18253.2017.1314555.

[25] M. Rimaz, J. Khalafy, H. Mousavi, S. Bohlooli, B. Khalili, Two Different Green Catalytic Systems for One-Pot Regioselective and Chemoselective Synthesis of Some Pyrimido[4,5-d]Pyrimidinone Derivatives in Water, J. Heterocycl. Chem. 54 (6) (2017) 3174–3186, https://doi.org/10.1002/jhet.2932.

[26] H.M. Zaheri, S. Javanshir, B. Hemmati, Z. Dolatkhah, M. Fardpour, Magnetic core–shell Carrageenan moss/Fe_3O_4: a polysaccharide-based metallic nanoparticles for synthesis of pyrimidinone derivatives via Biginelli reaction, Chem. Cent. J. 12 (108) (2018) 1–12, https://doi.org/10.1186/s13065-018-0477-3.

[27] S.F. Taheri Hatkehlouei, B. Mirza, S. Soleimani-Amiri, Solvent-Free One-Pot Synthesis of Diverse Dihydropyrimidinones/Tetrahydropyrimidinones Using Biginelli Reaction Catalyzed by Fe_3O_4@C@OSO_3H, Polycyclic Aromat. Compd. 42 (4) (2022) 1341–1357.

[28] A. Farhadi, J. Noei, R.H. Aliyari, M. Albakhtiyari, M.A. Takassi, Experimental and Theoretical Study on a One-Pot, Three-Component Route to 3,4-Dihydropyrimidin-2(1H)-Ones/Thiones $TiCl_3OTf$-[Bmim]Cl, Res. Chem. Intermed. 42 (2016) 1401–1409, https://doi.org/10.1007/s11164-015-2092-4.

[29] J.T. Starcevich, T.J. Laughlin, R.S. Mohan, Iron (III) Tosylate Catalyzed Synthesis of 3,4-Dihydropyrimidin-2(1H)-Ones/Thiones via the Biginelli Reaction, Tetrahedron Lett. 54 (8) (2013) 983–985, https://doi.org/10.1016/j.tetlet.2012.12.032.

[30] S. Zheng, Y. Jian, S. Xu, Y.a. Wu, H. Sun, G. Zhang, W. Zhang, Z. Gao, N-Donor ligand activation of titanocene for the Biginelli reaction via the imine mechanism, RSC Adv. 8 (16) (2018) 8657–8661.

[31] S. Sajjadifar, I. Amini, G. Mansouri, S. Alimohammadi, Fe_3O_4@APTES@isatin-SO_3H as heterogeneous and efficient catalyst for the synthesis of quinoxaline derivatives, Eurasian Chem. Commun. 2 (5) (2020) 626–633, https://doi.org/10.33945/SAMI/ECC.2020.5.9.

[32] A. Jalaeian-Hadad, A. Davoodnia, N. Tavakoli-Hoseini, F. Tajfirooz, Magnetically separable modified sulfuric acid ($CuFe_2O_4$@SiO_2-OSO_3H): Preparation, characterization, and catalytic application for the synthesis of 1,8-dioxo-octahydroxanthenes. Eurasian, Chem. Commun. 1 (6) (2019) 559–570, https://doi.org/10.33945/SAMI/ECC.2019.6.6.

[33] M. Hussein, N. Al-Lami, O.H.R. Al-Jeilawi, Design, Synthesis of Imidazolone and Oxazepine Derivatives Bearing Imidazo (2, 1-b) Thiazole along with its Antimicrobial Activity, Chem. Methodol. 6 (4) (2022) 319–330, https://doi.org/10.22034/chemm.2022.329943.1443.

[34] E. Haddazadeh, M. Mohammadi, One-pot Synthesize of Phenyl Phenanthro Imidazole Derivatives Catalyzed by Lewis Acid in the Presence of Ammonium Acetate, Chem. Methodol. 4 (3) (2020) 324–332, https://doi.org/10.33945/SAMI/CHEMM/2020.3.9.

[35] H. Ahankar, A. Ramazani, K. Ślepokura, T. Lis, V. Kinzhybalo, Magnetic cobalt ferrite nanoparticles functionalized with citric acid as a green nanocatalyst for one-pot three-component sonochemical synthesis of substituted 3-pyrrolin-2-ones, Res Chem Intermed. 45 (2019) 5007–5025, https://doi.org/10.1007/s11164-019-03878-1.

[36] H. Aghahosseini, A. Ramazani, K. Ślepokura, T. Lis, The first protection-free synthesis of magnetic bifunctional l -proline as a highly active and versatile artificial enzyme: Synthesis of imidazole derivatives, J. Colloid Interface Sci. 511 (2018) 222–232, https://doi.org/10.1016/j.jcis.2017.10.020.

[37] M.H.M. Al-Dahlaki, S.M.H. Al-Majidi, Synthesis and Study Impaction Antibacterial, Antifungal Activity Newly Pyridazine and 1,2,4-Triazine Derivatives, Chem. Methodol. 6 (4) (2022) 269–279. https://doi.org/10.22034/chemm.2022.320935.1412.

[38] S.R. Chowdhury, J.C. Bhangoji, T. Maiyalagan, S.S. Shendage, Ternary Al–Mg–Ag alloy promoted palladium nanoparticles as potential catalyst for enhanced electro-oxidation of ethanol, Int. J. Hydrog. Energy 46 (5) (2021) 4036–4044, https://doi.org/10.1016/j.ijhydene.2020.11.005.

[39] P.A. Kulkarni, A.K. Satpati, M. Thandavarayan, S.S. Shendage, An efficient Cu/functionalized graphene oxide catalyst for synthesis of 5-substituted 1H-tetrazoles, Chem. Pap. 75 (6) (2021) 2891–2899, https://doi.org/10.1007/s11696-021-01506-0.

[40] R.S. Shelkar, S.S. Shendage, J.M. Nagarkar, Ligand-free C-C and C–N cross-couplings with Pd/Nf-G nanocomposite, Tetrahedron Lett. 56 (30) (2015) 4463–4467, https://doi.org/10.1016/j.tetlet.2015.05.091.

[41] V.R. Nair, T. Maiyalagan, S.S. Shendage, Halloysite clay nanotubes with Fe–Al deposits forthe oxidation of benzyl alcohol, New J. Chem. 46 (2022) 17213–17222, https://doi.org/10.1039/D2NJ02742A.

[42] S.S. Kahandal, A.S. Burange, S.R. Kale, P. Prinsen, R. Luque, R.V. Jayaram, An efficient route to 1,8-dioxo-octahydroxanthenes and -decahydroacridines using a sulfated zirconia catalyst, Catal. Commun. 97 (2017) 138–145, https://doi.org/10.1016/j.catcom.2017.03.017.

[43] S.R. Kale, S.S. Kahandal, M.B. Gawande, R.V. Jayaram, Magnetically recyclable γ-Fe_2O_3–HAP nanoparticles for the cycloaddition reaction of alkynes, halides and azides in aqueous media, RSC Adv. 3 (2013) 8184–8192, https://doi.org/10.1039/C3RA00038A.

[44] A. Nagvenkar, S. Naik, J. Fernandes, Zinc oxide as a solid acid catalyst for esterification reaction, Catal. Commun. 65 (2015) 20–23, https://doi.org/10.1016/j.catcom.2015.02.009.

[45] A. Bayat, M. Shakourian-Fard, N. Ehyaei, M. Mahmoodi Hashemi, Silver nanoparticles supported on silica-coated ferrite as magnetic and reusable catalysts

for oxidant-free alcohol dehydrogenation, RSC Adv. 5 (2015) 22503–22509, https://doi.org/10.1039/C4RA15498C.

[46] S. Mahdjoub, R. Boulcina, M. Yildirim, S. Lakehal, H. Boulebd, A. Debache, A silver nanoparticles-catalyzed efficient three-component synthesis of polysubstituted 4 H -chromenylphosphonates and their antioxidant activity, Synthetic Communications 48 (18) (2018) 2366–2381.

[47] Z. Wang, H. Zhu, X. Wang, F. Yang, X. Yang, One-pot green synthesis of biocompatible arginine-stabilized magnetic nanoparticles, Nanotechnology 20 (46) (2009) 465606.

[48] V. Alfredo Reyes Villegas, J. Isaías De León Ramírez, E. Hernandez Guevara, S. Perez Sicairos, L. Angelica Hurtado Ayala, B. Landeros Sanchez, Synthesis and characterization of magnetite nanoparticles for photocatalysis of nitrobenzene, Journal of Saudi Chemical Society 24 (2) (2020) 223–235.

[49] M. Aslam, E.A. Schultz, T. Sun, T. Meade, V.P. Dravid, Synthesis of Amine-Stabilized Aqueous Colloidal Iron Oxide Nanoparticles, Cryst. Growth Des. 7 (3) (2007) 471–475, https://doi.org/10.1021/cg060656p.

[50] A. Manikandan, M. Durka, S.A. Antony, Magnetically Recyclable Spinel $Mn_xZn_{1-x}Fe_2O_4$ ($0.0 \leq x \leq 0.5$) Nano-Photocatalysts, Adv. Sci. Eng. Med. 7 (2015) 33–46, https://doi.org/10.1166/asem.2015.1654.

[51] M. Yamaura, R. Camilo, L. Sampaio, M. Macêdo, M. Nakamura, H. Toma, Preparation and characterization of (3-aminopropyl) triethoxysilane-coated magnetite nanoparticles, J. Magn. Magn. Mater. 279 (2–3) (2004) 210–217, https://doi.org/10.1016/j.jmmm.2004.01.094.

[52] B. Lesiak, N. Rangam, P. Jiricek, I. Gordeev, J. Tóth, L. Kövér, M. Mohai, P. Borowicz, Surface Study of Fe_3O_4 Nanoparticles Functionalized With Biocompatible Adsorbed Molecules, Front. Chem. 7 (2019) 642, https://doi.org/10.3389/fchem.2019.00642.

[53] S. Bhunia, S.K. Srivastava, A. Materny, A.K. Ojha, A vibrational and conformational characterization of arginine at different pH values investigated using Raman spectroscopy combined with DFT calculations, J. Raman Spectrosc. 47 (2016) 1073–1085, https://doi.org/10.1002/jrs.4918.

[54] A.J. Kora, J. Arunachalam, Green Fabrication of Silver Nanoparticles by Gum Tragacanth (Astragalus gummifer): A Dual Functional Reductant and Stabilizer, Journal of Nanomaterials 2012 (2012) 1–8.

[55] F. Wu, D. Liu, T. Wang, W. Li, X. Zhou, Different surface properties of L-arginine functionalized silver nanoparticles and their influence on the conductive and adhesive properties of nanosilver films, J. Mater. Sci. Mater. Electron. 26 (9) (2015) 6781–6786, https://doi.org/10.1007/s10854-015-3289-4.

[56] S.S. Patil, M.G. Mali, M.S. Tamboli, D.R. Patil, M.V. Kulkarni, H. Yoon, H. Kim, S. S. Al-Deyab, S.S. Yoon, S.S. Kolekar, B.B. Kale, Green approach for hierarchical nanostructured Ag-ZnO and their photocatalytic performance under sunlight, Catal. Today 260 (2016) 126–134, https://doi.org/10.1016/j.cattod.2015.06.004.

[57] J. Das, S.K. Pradhan, D.R. Sahu, D.K. Mishra, S.N. Sarangi, B.B. Nayak, S. Verma, B. K. Roul, Micro-Raman and XPS studies of pure ZnO ceramics, Physica B: Condensed Matter 405 (10) (2010) 2492–2497, https://doi.org/10.1016/j.physb.2010.03.020.

[58] W.-P. Mai, G.-C. Sun, J.-T. Wang, G.e. Song, P.u. Mao, L.-R. Yang, J.-W. Yuan, Y.-M. Xiao, L.-B. Qu, Silver-Catalyzed Radical Tandem Cyclization: An Approach to Direct Synthesis of 3-Acyl-4-arylquinolin-2(1H)-ones, J. Org. Chem. 79 (17) (2014) 8094–8102.

[59] M. Puripat, R. Ramozzi, M. Hatanaka, W. Parasuk, V. Parasuk, K. Morokuma, The Biginelli Reaction Is a Urea-Catalyzed Organocatalytic Multicomponent Reaction, J. Org. Chem. 80 (14) (2015) 6959–6967, https://doi.org/10.1021/acs.joc.5b00407.